J. Fluid Mech. (1972), *vol.* 51, *part* 2, *pp.* 363–383
Printed in Great Britain

Laminar dispersion in curved tubes and channels

By R. J. NUNGE, T.-S. LIN AND W. N. GILL†

Department of Chemical Engineering, Clarkson College of Technology, Potsdam, New York

(Received 26 March 1969 and in revised form 6 July 1971)

Dispersion in curved tubes and channels is treated analytically, using the velocity distribution of Topakoglu (1967) for tubes and that of Goldstein (1965) for curved channels. The result for curved tubes is compared with that obtained previously by Erdogan & Chatwin (1967) and it is found that the present dispersion coefficient contains the Erdogan & Chatwin result as a limiting case.

The most striking difference between the results is that Erdogan & Chatwin predict that the dispersion coefficient is always decreased by curvature if the Schmidt number exceeds 0·124, which is the case for essentially all systems of practical interest. In contrast, the present result, equation (76), predicts that the dispersion coefficient may be increased substantially by curvature in low Reynolds number flows, particularly in liquid systems which would be of interest in biological systems.

Two competing mechanisms of dispersion are present in curved systems. Curvature increases the variation in residence time across the flow in comparison with straight systems and this in turn increases the dispersion coefficient. The secondary flow which occurs in curved tubes creates a transverse mixing which decreases the dispersion coefficient. The results demonstrate that the relative importance of these two effects changes with the Reynolds number, since the dispersion coefficient first increases and then decreases as the Reynolds number increases. Since secondary flows are not present in curved channels the dispersion coefficient is increased over that in straight channels for all cases.

1. Introduction

The problem of the dispersion of a solute in laminar flow through ducts which produce straight streamlines has been investigated in a series of papers by Gill and coworkers (Gill 1967*a*, *b*; Gill & Anathakrishnan 1967; Gill, Ananthakrishnan & Nunge 1968; Sankarasubramanian & Gill 1971). Recently Gill & Sankarasubramanian (1970, 1971) presented an exact analysis of the unsteady convective diffusion equation and Chatwin (1970) investigated the approach to the asymptotic dispersion model.

Erdogan & Chatwin (1967) treated the problem of dispersion in curved tubes in a manner similar to that developed by Taylor (1953, 1954*a*, *b*) for straight tubes using the velocity distribution obtained by Dean (1927, 1928). McConalogue

† Present address: Faculty of Engineering and Applied Science, State University of New York at Buffalo.

(1970) developed an extended version of the velocity distribution in curved tubes which is valid for larger Dean numbers and used this to solve the dispersion problem in cases where molecular diffusion can be ignored. Both of these studies indicate that axial dispersion is decreased by the secondary flow present in curved tubes, although Erdogan & Chatwin found that the Schmidt number must exceed 0·124 for this result to hold.

Certain limiting assumptions were made in these studies and it is the purpose of this work to relax these assumptions and thus to provide a more complete description of the dispersion process in curved tubes, particularly in the low Reynolds number range for small values of the curvature. The curved channel system, which has not been investigated previously, provides an interesting case for comparison since flow in this geometry is not complicated by the presence of a secondary flow.

The analytical solution of the convective diffusion equation developed by Gill includes flows having both angular and time dependence. The method will be extended here to include the curved tube and channel geometries. Furthermore, the velocity distribution obtained by Topakoglu (1967) will be employed in the curved tube model such that the assumption made by Dean and used later by Erdogan & Chatwin and McConalogue, that the ratio of the tube radius to the radius of curvature is much less than unity, can be relaxed.

The most important feature of the theory of dispersion as introduced by Taylor (1953) is that it enables one to describe the average concentration distribution in a complex three-dimensional system by the solution of the one-dimensional convective diffusion equation. Then the primary problems are first to determine from first principles the dispersion coefficient associated with the one-dimensional dispersion equation and second to determine when the one-dimensional dispersion equation is a valid approximation.

2. Analysis

2.1. *Formulation of the dispersion model*

In the development for a binary system which follows, it is assumed that the bounding walls are parallel and impenetrable, the density of the mixture is constant, the fluid is incompressible and has a velocity independent of the coordinate in the main flow direction. The convective diffusion equation which describes the local concentration C' of solute in operator form becomes

$$\partial C'/\partial t + \nabla . \mathbf{v}C' = \nabla . D\nabla C', \tag{1}$$

where D is the molecular diffusion coefficient. Let V = a fixed volume in space bounded by the walls of the conduit and two planes which are perpendicular to the main flow direction, A = surface area of V, A_x = the cross-sectional area of the conduit perpendicular to the main flow direction, and $\mathbf{n}$ = unit normal vector to A, directed outward. By integrating (1) over V and applying the divergence theorem one gets

$$\frac{\partial}{\partial t}\int_V C'\,dV = \int_A (D\nabla C' - \mathbf{v}C').\mathbf{n}\,dA. \tag{2}$$

To put this result into a more useful form consider the orthogonal co-ordinate system (q_1, q_2, q_3) where q_2 is the co-ordinate in the main flow direction and h_1, h_2, h_3 are the associated metrical coefficients. The metrical coefficients are independent of q_2 because the cross-sectional area does not change in the flow direction. Thus

$$dV = h_1 h_2 h_3 dq_1 dq_2 dq_3 = S(q_1, q_3)\, dq_2 dA_x. \tag{3}$$

In this notation, q_2 is assumed to have dimensions of length and S is dimensionless. Because the bounding walls are solid and impenetrable, the velocity $\mathbf{v}$ and the mass flux in the direction parallel to $\mathbf{n}$ vanish at the walls. Thus the argument of the integral on the right-hand side of (2) vanishes at the walls and the only contributions to the surface area integration are obtained from integrating over the cross-sectional areas.

Substituting (3) in (2) and using the arguments above to simplify the right-hand side leads to

$$\frac{\partial}{\partial t}\int_{q_2}^{q_2+\Delta q_2}\int_{A_x} S(q_1, q_3,)\, C'\, dA_x dq_2 = \int_{A_x}\left(\frac{D}{S}\frac{\partial C'}{\partial q_2} - v_{q_2} C'\right) dA_x, \tag{4}$$

where v_{q_2} is the component of $\mathbf{v}$ in the q_2 direction. The result of differentiating (4) with respect to q_2 and assuming D is constant is

$$\frac{\partial}{\partial t}\int_{A_x} SC'\, dA_x = D\frac{\partial^2}{\partial q_2^2}\int_{A_x}\frac{C'}{S}\, dA_x - \frac{\partial}{\partial q_2}\int_{A_x} v_{q_2} C'\, dA_x. \tag{5}$$

Now define a new co-ordinate in the main flow direction moving with the average velocity as

$$\bar{q}_2 = q_2 - v_{q_2 m} t, \tag{6}$$

where

$$v_{q_2 m} = \int_{A_x} v_{q_2} dA_x \Big/ \int_{A_x} dA_x. \tag{7}$$

Equation (5), in the $(t, q_1, \bar{q}_2, q_3)$ co-ordinate system, becomes

$$\frac{\partial}{\partial t}\int_{A_x} SC'\, dA_x = v_{q_2 m}\frac{\partial}{\partial \bar{q}_2}\int_{A_x} SC'\, dA_x - \frac{\partial}{\partial \bar{q}_2}\int_{A_x} v_{q_2} C'\, dA_x + D\frac{\partial^2}{\partial \bar{q}_2^2}\int_{A_x}\frac{C'}{S}\, dA_x. \tag{8}$$

Define the volume average concentration $\bar{C}'$ in an element of length dq_2 in the flow direction as

$$\bar{C}' = d\left(q_2\int_{A_x} SC'\, dA_x\right)\Big/ d\left(q_2\int S\, dA_x\right) = \frac{1}{B}\int_{A_x} SC'\, dA_x. \tag{9}$$

Using this definition, (8) can be written as

$$\frac{\partial \bar{C}'}{\partial t} = v_{q_2 m}\frac{\partial \bar{C}'}{\partial \bar{q}_2} - \frac{1}{B}\frac{\partial}{\partial \bar{q}_2}\int_{A_x} v_{q_2} C'\, dA_x + \frac{D}{B}\frac{\partial^2}{\partial \bar{q}_2^2}\int_{A_x}\frac{C'}{S}\, dA_x. \tag{10}$$

The solution of (10) is now formulated (Gill & Sankarasubramanian 1970) as

$$C' = \bar{C}' + \sum_{j=1}^{\infty} F_j(t, q_1, q_3)\frac{\partial^j \bar{C}'}{\partial \bar{q}_2^j}. \tag{11}$$

By substituting (11) in (10) and rearranging, one has

$$\frac{\partial \bar{C}'}{\partial t} = v_{q_2 m}\left(1-\frac{A_x}{B}\right)\frac{\partial \bar{C}'}{\partial \bar{q}_2}+\frac{1}{B}\left(D\int_{A_x}\frac{dA_x}{S}-\int_{A_x} v_{q_2}F_1 dA_x\right)\frac{\partial^2 \bar{C}'}{\partial \bar{q}_2^2} + \frac{1}{B}\sum_{j=1}^{\infty}\frac{\partial^{j+2}\bar{C}'}{\partial \bar{q}_2^{j+2}}\left(D\int_{A_x}\frac{F_j}{S}dA_x-\int_{A_x} v_{q_2}F_{j+1}dA_x\right). \tag{12}$$

Equation (12) is in the form of the generalized dispersion model with time-dependent coefficients, which for this problem is

$$\frac{\partial \bar{C}'}{\partial t} = \sum_{i=1}^{\infty} k_i(t)\frac{\partial^i \bar{C}'}{\partial \bar{q}_2^i}. \tag{13}$$

Upon comparing (12) and (13), the dispersion coefficients k_i are given by

$$k_1 = v_{q_2 m}(1-A_x/B), \tag{14a}$$

$$k_2 = \frac{1}{B}\left(D\int_{A_x}\frac{dA_x}{S}-\int_{A_x} v_{q_2}F_1 dA_x\right), \tag{14b}$$

$$k_{i+2} = \frac{1}{B}\left[D\int_{A_x}\frac{F_j}{S}dA_x-\int_{A_x} v_{q_2}F_{j+1}dA_x\right] \quad (i = 1, 2, \ldots). \tag{14c}$$

For straight circular tubes these expressions reduce to those given by Gill & Sankarasubramanian (1970). A development for the curved tube geometry which demonstrates the details of calculating the dispersion coefficients is given in what follows.

2.2. *Curved tube system*

In the co-ordinate system shown in figure 1 the co-ordinates r, $R\theta$ and $a\phi$ are identified with q_1, q_2 and q_3 respectively. It is easily demonstrated that k_1 reduces to zero in curved tubes and channels. For example, in a curved tube of radius a and radius of curvature R

$$B = \int_0^{2\pi}\int_0^a\left(1+\frac{r}{R}\cos\phi\right)r\,dr\,d\phi = A_x$$

and hence (14a) yields $k_1 = 0$.

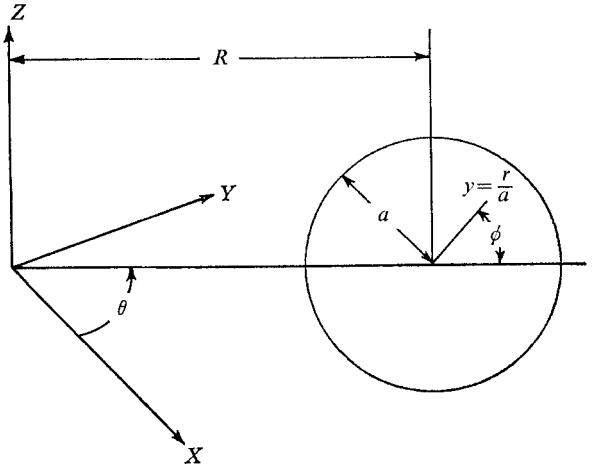

FIGURE 1. Schematic diagram of the curved tube.

In dimensionless form, the equations of continuity and motion for steady, fully developed flow of a constant property fluid are

$$\frac{\partial u}{\partial y}+\frac{u\cos\phi}{\lambda+y\cos\phi}+\frac{u}{y}+\frac{1}{y}\frac{\partial v}{\partial\phi}-\frac{v\sin\phi}{\lambda+y\cos\phi}=0, \tag{15}$$

$$u\frac{\partial u}{\partial y}-\frac{v^2}{y}+\frac{v}{y}\frac{\partial u}{\partial\phi}-\frac{w^2\cos\phi}{\lambda+y\cos\phi}=-\frac{\partial p}{\partial y}-\frac{1}{Re}\left[\left(\frac{1}{y}\frac{\partial}{\partial\phi}-\frac{\sin\phi}{\lambda+y\cos\phi}\right)\left(\frac{\partial v}{\partial y}+\frac{v}{y}-\frac{1}{y}\frac{\partial u}{\partial\phi}\right)\right], \tag{16}$$

$$u\frac{\partial v}{\partial y}+\frac{uv}{y}+\frac{v}{y}\frac{\partial v}{\partial\phi}+\frac{w^2\sin\phi}{\lambda+y\cos\phi}=-\frac{1}{y}\frac{\partial p}{\partial\phi}+\frac{1}{Re}\left[\left(\frac{\partial}{\partial y}+\frac{\cos\phi}{\lambda+y\cos\phi}\right)\left(\frac{\partial v}{\partial y}+\frac{v}{y}-\frac{1}{y}\frac{\partial u}{\partial\phi}\right)\right], \tag{17}$$

$$u\frac{\partial w}{\partial y}+\frac{uw\cos\phi}{\lambda+y\cos\phi}+\frac{v}{y}\frac{\partial w}{\partial\phi}-\frac{vw\sin\phi}{\lambda+y\cos\phi}=-\frac{1}{(\lambda+y\cos\phi)}\frac{\partial p}{\partial\theta}$$
$$+\frac{1}{Re}\left[\left(\frac{\partial}{\partial y}+\frac{1}{y}\right)\left(\frac{\partial w}{\partial y}+\frac{w\cos\phi}{\lambda+y\cos\phi}\right)+\frac{1}{y}\frac{\partial}{\partial\phi}\left(\frac{1}{y}\frac{\partial w}{\partial\phi}-\frac{w\sin\phi}{\lambda+y\cos\phi}\right)\right]. \tag{18}$$

Here u, w and v are the dimensionless velocity components corresponding to (r,θ,ϕ) respectively with W_0, the centre-line velocity in a straight pipe with a radius a and the same pressure gradient as exists along the centre-line in the curved pipe, used as a reference. Additional dimensionless quantities include $y=r/a$, $\lambda=R/a$, $Re=W_0a/\nu$, $p=P/\rho W_0^2$. Upon recognizing that the boundary conditions introduce no further parameters, the functional dependence of the velocity can be written as

$$\mathbf{v}=\mathbf{v}(y,\phi,\lambda,Re). \tag{19}$$

Dean (1927, 1928) and McConologue & Srivastava (1968) solved these equations for the special case of

$$\lambda^{-1}\ll 1, \tag{20}$$

that is, the case when the ratio of the tube radius to the radius of curvature is very small. This assumption brings about a considerable reduction in the number of terms retained in the equations since it allows the following simplifications:

$$\frac{\partial}{\partial y}+\frac{\cos\phi}{\lambda+y\cos\phi}\cong\frac{\partial}{\partial y}, \tag{21}$$

$$\frac{1}{y}\frac{\partial}{\partial\phi}-\frac{\sin\phi}{\lambda+y\cos\phi}\cong\frac{1}{y}\frac{\partial}{\partial\phi}, \tag{22}$$

$$\lambda+y\cos\phi\cong\lambda. \tag{23}$$

Because of these simplifications the parameters λ and Re of the original problem are combined into a single parameter $\lambda^{-1}Re^2$ which is called the Dean number.

Topakoglu (1967) avoided this assumption and solved the complete set of equations by introducing a stream function ψ and expanding both w and ψ in a series using λ^{-1} as the perturbation parameter. The zero-order term in the series

for w is the parabolic profile for flow in a straight tube. The results given by Topakoglu are in the form

$$w(y,\phi,\lambda) = w_0(y) + \lambda^{-1}w_1(y,\phi) + \lambda^{-2}w_2(y,\phi) + \ldots, \tag{24a}$$

$$\psi(y,\phi,\lambda) = \psi_1(y,\phi) + \lambda^{-1}\psi_2(y,\phi) + \lambda^{-2}\psi_3(y,\phi) + \ldots, \tag{24b}$$

where $$u(y,\phi,\lambda) = -\frac{1}{y(\lambda + y\cos\phi)}\frac{\partial\psi}{\partial\phi}, \quad v(y,\phi,\lambda) = \frac{1}{(\lambda + y\cos\phi)}\frac{\partial\psi}{\partial y} \tag{24c}$$

and the functions necessary to solve the dispersion equation are given in the appendix.

In the (τ, y, θ, ϕ) system the dimensionless convective diffusion equation for the concentration C is

$$\frac{\partial C}{\partial\tau} + Pe\left[u\frac{\partial C}{\partial y} + \frac{v}{y}\frac{\partial C}{\partial\phi} + \frac{w}{\lambda + y\cos\phi}\frac{\partial C}{\partial\theta}\right] = \frac{1}{y}\frac{\partial}{\partial y}\left(y\frac{\partial C}{\partial y}\right) + \frac{\cos\phi}{\lambda + y\cos\phi}\frac{\partial C}{\partial y} + \frac{1}{y^2}\frac{\partial^2 C}{\partial\phi^2} - \frac{\sin\phi}{y(\lambda + y\cos\phi)}\frac{\partial C}{\partial\phi} + \frac{1}{(\lambda + y\cos\phi)^2}\frac{\partial^2 C}{\partial\theta^2}, \tag{25}$$

where $$Pe = W_0 a/D, \quad \tau = tD/a^2 \quad C = C'/C_0.$$

The system is assumed to be devoid of solute initially and at time zero a step change in solute concentration, $C' = C_0$, is introduced at $\theta = 0$. The initial and boundary conditions are thus

$$C(0,y,\phi,\theta) = 0, \quad C(\tau,y,\phi,0) = 1, \tag{26), (27}$$

$$\frac{\partial C}{\partial y}(\tau,1,\phi,\theta) = 0, \tag{28}$$

$$\frac{\partial C}{\partial\phi}(\tau,y,0,\theta) = \frac{\partial C}{\partial\phi}(\tau,y,\pi,\theta) = 0, \tag{29}$$

$$C(\tau,0,\phi,\theta) \quad \text{and} \quad \frac{\partial C}{\partial y}(\tau,0,\phi,\theta) \quad \text{finite.} \tag{30}$$

The assumption of equation (20) relating to the curvature, which enables one to use (21), (22) and (23), was employed by Erdogan & Chatwin (1967) to simplify the convective diffusion equation in a manner similar to that used for the equations of continuity and motion. Here we retain the complete convective diffusion equation (25).

The S function introduced in §2.1 is $1 + (r/R)\cos\phi$ for curved tubes. If the assumption related to the curvature is employed, then this reduces to unity, and $\bar{C}$ and the area average concentration are equal.

From the statement of the problem the functional dependence of the concentration can be written as

$$C = C(\tau, y, \phi, \theta, \lambda, Pe, Re). \tag{31}$$

Since the Péclet number Pe is the product of the Reynolds and Schmidt numbers, the Péclet number dependence may be replaced by the Schmidt number Sc in (31).

2.3. *Curved channel*

The curved channel, shown schematically in figure 2, is most conveniently treated in cylindrical co-ordinates. The convective diffusion equation and associated boundary conditions are

$$\frac{\partial C}{\partial \tau}+\frac{Pe}{y+\lambda}w\frac{\partial C}{\partial \theta}=\frac{1}{y+\lambda}\frac{\partial}{\partial y}\left[(y+\lambda)\frac{\partial C}{\partial y}\right]+\frac{1}{(y+\lambda)^2}\frac{\partial^2 C}{\partial \theta^2}, \tag{32}$$

$$C(0,y,\theta)=0, \quad C(\tau,y,0)=1, \tag{33), (34}$$

$$\frac{\partial C}{\partial y}(\tau,-1,\theta)=\frac{\partial C}{\partial y}(\tau,1,\theta)=0, \tag{35}$$

$$y=r/h-\lambda, \quad \lambda=R/h, Pe=hW_m/D.$$

For curved channels, the S function is r/R. If $\lambda \gg 1$, this reduces to unity and $\bar{C}$ reduces to the area average concentration.

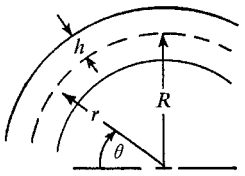

FIGURE 2. Schematic diagram of the curved channel.

The dimensionless velocity distribution using the mean velocity W_m as reference is given by Goldstein (1965) and may be written as

$$w=2(\lambda-1)\frac{\left\{\left[\frac{(\lambda+1)^2}{4\lambda}\ln\left(\frac{\lambda+1}{\lambda-1}\right)\right]\left[\frac{\lambda+y}{\lambda-1}-\frac{\lambda-1}{\lambda+y}\right]-\left(\frac{\lambda+y}{\lambda-1}\right)\ln\left(\frac{\lambda+y}{\lambda-1}\right)\right\}}{\left\{\lambda-\frac{(\lambda+1)^2(\lambda-1)^2}{4\lambda}\left[\ln\left(\frac{\lambda+1}{\lambda-1}\right)\right]^2\right\}}. \tag{36}$$

2.4. *Method of solution*

To generate the dispersion coefficients it is necessary to determine the F_j functions introduced in (11). Here we shall be concerned only with the large-time solution so that the dispersion model, truncated after two terms on the right-hand side of (13) such that the second derivative is the highest one retained, is an accurate representation of the results. Also, only the steady-state part of the dispersion coefficients are required. Higher-order coefficients and the time-dependent parts of the dispersion coefficients become tedious to calculate for curved tubes because the solution for the velocity distribution is in the form of a complicated series expansion.

Following the development given in §2.1, but introducing dimensionless groups, let the dimensionless counterpart of $\bar{q}_2$ be

$$X_1=(\lambda/Pe)\theta-w_m\tau, \tag{37}$$

where w_m is unity for the curved channel and

$$w_m = \frac{1}{\pi}\int_0^{2\pi}\int_0^1 yw\,dy\,d\phi \tag{38}$$

for the curved tube. Since the curved tube is the more important case we shall develop the dispersion model solution using this configuration. The curved channel problem is relatively straight-forward and only the important results will be given.

To solve (25), transform it to (τ, y, X_1, ϕ) co-ordinates and let

$$C = \bar{C} + \sum_{j=1}^{\infty} f_j(\tau, y, \phi)\frac{\partial^j \bar{C}}{\partial X_1^j}, \tag{39}$$

where the f_j's are the dimensionless counterparts of the F_j's in (11) and

$$\bar{C} = \frac{\int_0^{2\pi}\int_0^1 y(\lambda + y\cos\phi)\,C\,dy\,d\phi}{\int_0^{2\pi}\int_0^1 y(\lambda + y\cos\phi)\,dy\,d\phi}. \tag{40}$$

The process of distributing $\bar{C}$ is assumed to be described by

$$\frac{\partial \bar{C}}{\partial \tau} = \sum_{i=1}^{\infty} K_i \frac{\partial^i \bar{C}}{\partial X_1^i}, \tag{41}$$

which corresponds to (13) in dimensionless form. Only the truncated form of (41) will be considered here and since $K_1 = 0$,

$$\frac{\partial \bar{C}}{\partial \tau} = K_2 \frac{\partial^2 \bar{C}}{\partial X_1^2}. \tag{42}$$

Equation (42), together with an expression for K_2 derived from first principles, is the essence of the theory of dispersion. That is, under certain conditions which are frequently met in practice, (42) enables one to determine very simply the concentration distribution in a complex convective diffusion system. From (42),

$$\partial^{n+1}\bar{C}/\partial\tau\,\partial X_1^n = K_2\,\partial^{n+2}\bar{C}/\partial X_1^{n+2} \tag{43}$$

if K_2 is independent of X_1. Equations (42) and (43) become exact only asymptotically as $\tau \to \infty$. However, for straight tubes and parallel plates the region of validity of this assumption has been studied (Ananthakrishnan, Gill & Barduhn 1965; Gill & Ananthakrishnan 1966, 1967; Gill *et al.* 1968; Gill & Sankarasubramanian 1970) by both approximate and exact analytical, and exact numerical calculations, and criteria for the validity of (42) have been given. For example, with laminar flow for Péclet numbers > 100 in a tube with a step change in inlet concentration equation (42) is an excellent approximation if $tD/a^2 \gtrsim 0{\cdot}8$. It has also been shown (Gill & Ananthakrishnan 1966) that equation (39) is an accurate solution for the local concentration, C under the conditions for which (42) is valid. It will be shown later for the curved tube that equation (42) is a good approximation if $\tau \gtrsim 101K_2^{0{\cdot}9}$.

The problem of finding K_2 for flow in a curved tube is more complicated than for a straight tube because of the existence of transverse and angular convection currents in the former. However, this difficulty is overcome by the perturbation expansions in λ^{-1} which will be described subsequently.

After substituting (39), (42), and (43) in (25) and equating the cefficients of like derivatives of $\bar{C}$ with respect to X_1 to zero the following system of equations is generated.

$$\frac{\partial f_1}{\partial \tau}+Pe\left(u\frac{\partial f_1}{\partial y}+\frac{v}{y}\frac{\partial f_1}{\partial \phi}\right)+\lambda\left(\frac{w}{\lambda+y\cos\phi}-\frac{w_m}{\lambda}\right)=\frac{1}{y}\frac{\partial}{\partial y}\left(y\frac{\partial f_1}{\partial y}\right)+\frac{\cos\phi}{\lambda+y\cos\phi}\frac{\partial f_1}{\partial y}$$
$$+\frac{1}{y^2}\frac{\partial^2 f_1}{\partial \phi^2}-\frac{\sin\phi}{y(\lambda+y\cos\phi)}\frac{\partial f_1}{\partial \phi}, \tag{44}$$

$$\frac{\partial f_2}{\partial \tau}+Pe\left(u\frac{\partial f_2}{\partial y}+\frac{v}{y}\frac{\partial f_2}{\partial \phi}\right)+\lambda\left(\frac{w}{\lambda+y\cos\phi}-\frac{w_m}{\lambda}\right)f_1=\frac{1}{y}\frac{\partial}{\partial y}\left(y\frac{\partial f_2}{\partial y}\right)+\frac{\cos\phi}{\lambda+y\cos\phi}\frac{\partial f_2}{\partial y}$$
$$+\frac{1}{y^2}\frac{\partial^2 f_2}{\partial \phi^2}-\frac{\sin\phi}{y(\lambda+y\cos\phi)}\frac{\partial f_2}{\partial \phi}-K_2+\frac{(\lambda/Pe)^2}{(\lambda+y\cos\phi)^2}, \tag{45}$$

$$\frac{\partial f_{i+2}}{\partial \tau}+Pe\left(u\frac{\partial f_{i+2}}{\partial y}+\frac{v}{y}\frac{\partial f_{i+2}}{\partial \phi}\right)+\lambda\left(\frac{w}{\lambda+y\cos\phi}-\frac{w_m}{\lambda}\right)f_{i+1}=\frac{1}{y}\frac{\partial}{\partial y}\left(y\frac{\partial f_{i+2}}{\partial y}\right)$$
$$+\frac{\cos\phi}{\lambda+y\cos\phi}\frac{\partial f_{i+2}}{\partial y}+\frac{1}{y^2}\frac{\partial^2 f_{i+2}}{\partial \phi^2}-\frac{\sin\phi}{y(\lambda+y\cos\phi)}\frac{\partial f_{i+2}}{\partial \phi}-\left[K_2-\frac{(\lambda/Pe)^2}{(\lambda+y\cos\phi)^2}\right]f_i$$
$$(i=1,2,\ldots). \tag{46}$$

The initial and boundary conditions become

$$f_i(0,y,\phi)=0, \tag{47}$$

$$\frac{\partial f_i}{\partial y}(\tau,1,\phi)=0, \tag{48}$$

$$\frac{\partial f_i}{\partial \phi}(\tau,y,0)=\frac{\partial f_i}{\partial \phi}(\tau,y,\pi)=0, \tag{49}$$

and the condition that

$$\int_0^{2\pi}\int_0^1 y(\lambda+y\cos\phi)f_i\,dy\,d\phi=0 \tag{50}$$

follows from (39) and (40).

The solutions of (44) –(46) are now formulated as

$$f_1=f_{s_1}(y,\phi)+h_1(\tau,y,\phi), \tag{51}$$

$$f_2=f_{s_2}(y,\phi)+h_2(\tau,y,\phi), \tag{52}$$

$$f_{i+2}=f_{s_{i+2}}(\tau,y,\phi)+h_{i+2}(\tau,y,\phi), \tag{53}$$

where the h functions account for the transients which vanish as τ grows large. Up to this point the solution of the curved channel system parallels that of the curved tube. However, because the velocity distribution for the tube is given in the form of a series expansion in λ^{-1} it is now necessary to formulate the f_s functions and the dispersion coefficient as

$$f_{s_1}=\sum_{n=0}^{\infty}\lambda^{-n}g_{1n}, \tag{54}$$

$$f_{s_2}=\sum_{n=0}^{\infty}\lambda^{-n}g_{2n}, \tag{55}$$

$$K_2=\sum_{n=0}^{\infty}\lambda^{-n}K_{2n}. \tag{56}$$

This step is not needed for the curved channel since the velocity distribution is given in closed form. It will be shown below that three terms in the expansions for the f_s functions are sufficient to calculate the first three terms in the expansion for K_2. Since only three terms in the velocity distribution are available at present, it would require considerably more effort to extend the calculation of K_2.

To find the dispersion coefficient the f_{s_1} function is required. On substituting (51), (24*a*), (24*b*), (24*c*), and (54) into (44) and considering only the time-independent part, multiplying through by $(\lambda + y\cos\phi)$ and equating coefficients of like powers of λ to zero one has

$$w_0 - w_{0_m} = \nabla^2 g_{10}, \tag{57}$$

$$\frac{ReSc}{y}\left[-\frac{\partial\psi_1}{\partial\phi}\frac{\partial g_{10}}{\partial y}+\frac{\partial\psi_1}{\partial y}\frac{\partial g_{10}}{\partial\phi}\right]+w_1-w_{1_m}-y\cos\phi\, w_{0_m}-\cos\phi\frac{\partial g_{10}}{\partial y}+\frac{\sin\phi}{y}\frac{\partial g_{10}}{\partial\phi}$$
$$-y\cos\phi\,\nabla^2 g_{10}=\nabla^2 g_{11}, \tag{58}$$

$$\frac{ReSc}{y}\left[-\frac{\partial\psi_1}{\partial\phi}\frac{\partial g_{11}}{\partial y}+\frac{\partial\psi_1}{\partial y}\frac{\partial g_{11}}{\partial\phi}-\frac{\partial\psi_2}{\partial\phi}\frac{\partial g_{10}}{\partial y}+\frac{\partial\psi_2}{\partial y}\frac{\partial g_{10}}{\partial\phi}\right]+w_2-w_{2_m}-y\cos\phi\, w_{1_m}$$
$$-\cos\phi\frac{\partial g_{11}}{\partial y}+\frac{\sin\phi}{y}\frac{\partial g_{11}}{\partial\phi}-y\cos\phi\,\nabla^2 g_{11}=\nabla^2 g_{12}. \tag{59}$$

Here
$$\nabla^2=\frac{1}{y}\frac{\partial}{\partial y}\left(y\frac{\partial}{\partial y}\right)+\frac{1}{y^2}\frac{\partial^2}{\partial\phi^2}. \tag{60}$$

Higher order functions may be obtained similarly; second-order functions are sufficient for our purposes here.

Since g_{10} is the counterpart of the straight pipe solution,

$$g_{10}=\tfrac{1}{8}(-\tfrac{1}{3}+y^2-\tfrac{1}{2}y^4). \tag{61}$$

Equation (58) can be rewritten in the form

$$\nabla^2 g_{11}=L_{11}(y)\cos\phi$$

and hence the solution is of the form

$$g_{11}=G_{11}(y)\cos\phi+G_1(y), \tag{62}$$

where G_1 is identically zero and L_{11} and G_{11} are given in the appendix. In a similar manner (59) can be written

$$\nabla^2 g_{12}=L_{12}(y)\cos 2\phi+L_1(y)$$

and
$$g_{12}=G_{12}(y)\cos 2\phi+G_2(y), \tag{63}$$

with L_1 and G_2 tabulated in the appendix.

With three terms in the f_{s_1} function known it is possible to compute the first three terms in the dispersion coefficient expansion. Upon substituting (51), (52), (24*a*), (24*b*), (24*c*), (54) and (55) into (45), considering only the time-independent part, and multiplying through by $(\lambda + y\cos\phi)^2$ and equating coefficients

of like powers of λ to zero, one obtains for g_{20}, g_{21} and g_{22}

$$K_{20} - (1/Pe^2) + (w_0 - w_{0m})\, g_{10} = \nabla^2 g_{20}, \tag{64}$$

$$K_{21} + 2y\cos\phi\, K_{20} + (w_1 - w_{1m} + y w_0 \cos\phi - 2y\cos\phi w_{0m})\, g_{10} + (w_0 - w_{0m})\, g_{11}$$
$$+ \frac{ReSc}{y}\left(-\frac{\partial\psi_1}{\partial\phi}\frac{\partial g_{20}}{\partial y} + \frac{\partial\psi_1}{\partial y}\frac{\partial g_{20}}{\partial\phi}\right) - 2y\cos\phi\nabla^2 g_{20} - \left(\cos\phi\frac{\partial g_{20}}{\partial y} - \frac{\sin\phi}{y}\frac{\partial g_{20}}{\partial\phi}\right) = \nabla^2 g_{21}, \tag{65}$$

$$K_{22} + 2y\cos\phi K_{21} + y^2\cos^2\phi K_{20} + (w_2 - w_{2m} + y\cos\phi w_1 - 2y\cos\phi w_{1m} - y^2 \cos^2\phi w_{0m})\, g_{10}$$
$$+ (w_1 - w_{1m} + y\cos\phi w_0 - 2y\cos\phi w_{0m})\, g_{11} + (w_0 - w_{0m})\, g_{12} + ReSc/y$$
$$\left(-\frac{\partial\psi_2}{\partial\phi}\frac{\partial g_{20}}{\partial y} + \frac{\partial\psi_2}{\partial y}\frac{\partial g_{20}}{\partial\phi} - \frac{\partial\psi_1}{\partial\phi}\frac{\partial g_{21}}{\partial y} + \frac{\partial\psi_1}{\partial y}\frac{\partial g_{21}}{\partial\phi}\right) + ReSc\cos\phi\left(-\frac{\partial\psi_1}{\partial\phi}\frac{\partial g_{20}}{\partial y} + \frac{\partial\psi_1}{\partial y}\frac{\partial g_{20}}{\partial\phi}\right)$$
$$- 2y\cos\phi\,\nabla^2 g_{21} - y^2\cos^2\phi\nabla^2 g_{20} - \left(\cos\phi\frac{\partial g_{21}}{\partial y} - \frac{\sin\phi}{y}\frac{\partial g_{21}}{\partial\phi}\right)$$
$$- y\cos\phi\left(\cos\phi\frac{\partial g_{20}}{\partial y} - \frac{\sin\phi}{y}\frac{\partial g_{20}}{\partial\phi}\right) = \nabla^2 g_{22}. \tag{66}$$

Since g_{20} is the counterpart of the straight pipe solution it is obtained immediately as

$$g_{20} = \frac{1}{16\times 8}\left(\tfrac{31}{360} - \tfrac{1}{2}y^2 + \tfrac{5}{6}y^4 - \tfrac{5}{9}y^6 + \tfrac{1}{8}y^8\right) \tag{67}$$

and

$$K_{20} = (1/Pe^2) + \tfrac{1}{192}. \tag{68}$$

Equation (65) can be rewritten in the form

$$\nabla^2 g_{21} = L_{21}(y)\cos\phi + K_{21}$$

and hence the solution is of the form

$$g_{21} = H_{21}(y)\cos\phi + H_1(y),$$

where

$$\frac{1}{y}\frac{d}{dy}\left(y\frac{dH_1}{dy}\right) = K_{21}.$$

The functions L_{21} and H_{21} are given in the appendix. In view of the boundary condition given by (48)

$$(dH_1/dy)_{y=1} = 0$$

and thus

$$K_{21} = 0. \tag{69}$$

It can also be demonstrated that H_1 vanishes.

Equation (66) can be rewritten in the form

$$\nabla^2 g_{22} = K_{22} + L_{22}(y)\cos 2\phi + L_2(y) \tag{70}$$

and hence

$$g_{22} = H_{22}(y)\cos 2\phi + H_2(y), \tag{71}$$

where

$$\frac{1}{y}\frac{d}{dy}\left(y\frac{dH_2}{dy}\right) = L_2(y) + K_{22}. \tag{72}$$

Since $(dH_2/dy)_{y=1} = 0$ integration of (72) yields

$$K_{22} = -2\int_0^1 yL_2(y)\,dy. \tag{73}$$

The function L_2 is listed in the appendix.

By proceeding in a manner similar to that used for the curved tube it is easily demonstrated that the dispersion coefficient for the curved channel is

$$K_2 = \frac{\lambda}{2Pe^2}\ln\frac{(\lambda+1)}{(\lambda-1)} - \frac{1}{2\lambda}\int_{-1}^{1}\{\lambda w-(y+\lambda)\}f_{s_1}(y)\,dy, \tag{74}$$

where

$$f_{s_1}(y) = \int_{-1}^{y}\frac{1}{\alpha+\lambda}\int_{-1}^{\alpha}\{\lambda w-(\sigma+\lambda)\}\,d\sigma\,d\alpha - \frac{1}{2\lambda}\int_{-1}^{1}(\lambda+y)\int_{-1}^{y}\frac{1}{\alpha+\lambda}\int_{-1}^{\alpha}\{\lambda w-(\sigma+\lambda)\}\,d\sigma\,d\alpha\,dy. \tag{75}$$

3. Results and discussion

Two competing mechanisms occur in curved systems and have opposite effects on the dispersion coefficient. First, curvature tends to increase the variation in residence times across the flow. This occurs because particles in any cross-section have different distances to travel to sweep out an angle θ and this increases K_2. In contrast, the circulation which occurs in curved tubes, but not in curved channels, creates transverse mixing which decreases the dispersion coefficient.

3.1. *Curved tube*

The dispersion coefficient for the curved tube, based on the velocity distribution of Topakoglu, is calculated by the present approach to be

$$K_2 = \left(\frac{1}{Pe^2}+\frac{1}{192}\right) + \left\{\frac{4Re^4}{576^2\times 160}\left[-\frac{2569}{15\,840}Sc^2+\frac{109}{43\,200}\right] + \frac{2Re^2}{576\times 144}\left[\frac{31}{60}Sc-\frac{25\,497}{13\,440}\right] + \left[\frac{419}{8\times 15\times 96}+0{\cdot}25\left(\frac{1}{Pe^2}+\frac{1}{192}\right)\right]\right\}\lambda^{-2}. \tag{76}$$

Equation (76) is obtained by substituting (68), (69) and (73) in (56) and ignoring terms containing λ raised to powers of -3 or less. It can be shown that using the same method and the velocity distribution of Dean one obtains

$$K_2 = \left(\frac{1}{Pe^2}+\frac{1}{192}\right) + \frac{4Re^4\lambda^{-2}}{576^2\times 160}\left[-\frac{2569}{15\,840}Sc^2+\frac{109}{43\,200}\right], \tag{77}$$

which is the same as that obtained by Erdogan & Chatwin and is contained in the result given by (76). That is, given a particular velocity distribution, the present approach and that of Erdogan & Chatwin yield the same expression for the dispersion coefficient. However, the present approach provides one with a more complete description of the concentration distribution.

Since K_2 is an even function of λ, the truncated series represents a one-term correction to the straight pipe case under a constant pressure gradient which is

correct to the third-order because $K_{23} = 0$. Hence, for the velocity distributions used, both (76) and (77) are correct to the third-order and the differences between them are due to differences in the velocity distribution used and the introduction of the simplifications of (21), (22) and (23) used in (25) to obtain (77). Comparison of (76) and (77) shows that the use of Dean's velocity distribution and these simplifications results in the loss of the last two terms in (76).

As is always the case the question of series convergence is important in determining the accuracy of the truncated result. However, to investigate the convergence it is necessary to find at least the K_{24} term in the expansion of K_2 given by (56). This would require the fourth- and fifth-order correction terms in the velocity and stream function expansions given by (24*a*) and (24*b*) which are not yet available.

The differences between (76) and (77) are due entirely to the velocity distributions used and the assumptions represented in (21), (22) and (23), and not to the methods employed to calculate K_2. Therefore, by comparing the predictions of the model used here, model NLG, and that of Erdogan & Chatwin, model EC, one can determine the values of the parameters for which the use of (21), (22), and (23) and the assumptions made in determining the velocity distribution are most critical in calculating the dispersion coefficient.

First, it should be noted that the terms of the coefficient of λ^{-2} in (76) are multiplied by Re^4, Re^2 and Re^0 respectively. Therefore, we may expect the Re^4 term to dominate at large Reynolds numbers in which case (76) and (77) would yield essentially the same results. Second, since for real physical systems the Schmidt number is always greater than 0·12, the Re^4 terms always decreases the dispersion coefficient. In constrast, the Re^0 term always increases the dispersion coefficient as does the Re^2 term if $Sc > 3{\cdot}7$. This leads to the most striking qualitative difference between models EC and NLG. Namely that the former predicts that transverse convection dominates and therefore the dispersion coefficient is decreased by curvature in essentially all physical situations of practical interest, while model NLG predicts that in low Reynolds numbers systems, and particularly in liquid systems, the dispersion coefficient may be increased substantially by curvature.

One can infer the physical mechanisms which contribute to the various terms in the coefficient of λ^{-2} in (76). The term involving Re^0, which always increases the dispersion coefficient, occurs because of axial molecular diffusion and elongation of the distribution of the velocity component in the direction of flow. The terms involving Re^2 and Re^4 reflect the competing effects of velocity profile elongation, which increases dispersion, and transverse mixing caused by the u and v components of velocity, which decreases it. At higher Reynolds numbers the Re^4 term dominates as does the effect of more intense transverse convection which occurs at higher Reynolds numbers. However, at lower Reynolds numbers the Re^2 term is more important and since transverse mixing is not as intense in this region the result is an increase in dispersion unless the Schmidt number is less than approximately 3·7.

To make comparisons between the two models, the results for models EC given in equation (3.16) of the paper by Erdogan & Chatwin (1967) which depend only

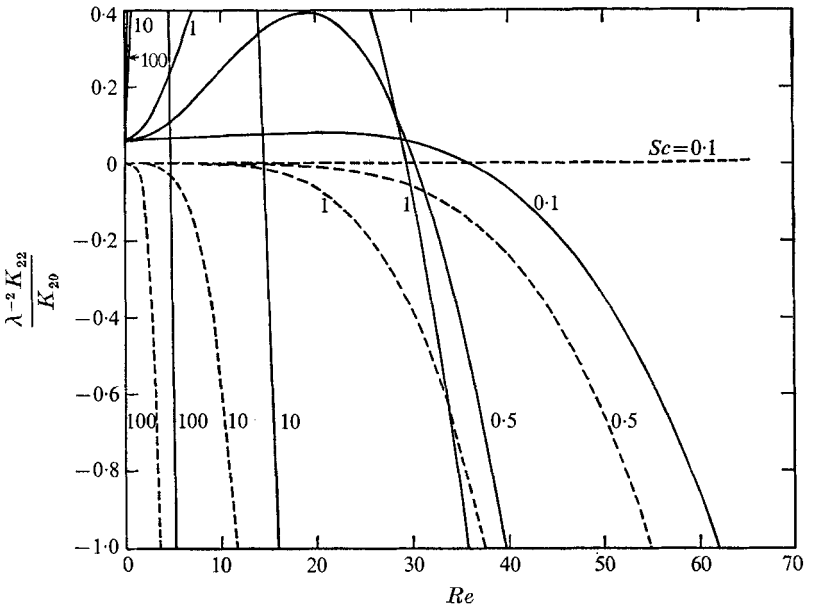

FIGURE 3. Curved tube correction to the dispersion coefficient normalized by the straight tube dispersion coefficient *vs.* Re for $\lambda = 2$ with Sc as parameter. – – –, Erdogan & Chatwin (1967); ———, this study.

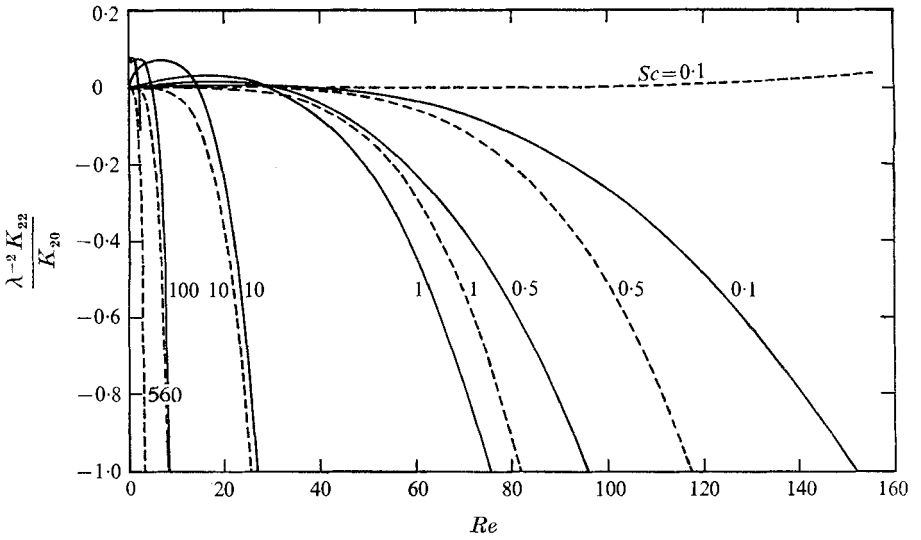

FIGURE 4. Curved tube correction to the dispersion coefficient normalized by the straight tube dispersion coefficient *vs.* Re for $\lambda = 10$ with Sc as a parameter. – – –, Erdogan & Chatwin (1967); ———, this study.

on the Dean and Schmidt numbers were converted to the three parameter system of this paper by breaking up the Dean number into the curvature ratio and the Reynolds number. These and the present results are plotted in figures 3 to 5 as the ratio $\lambda^{-2}K_{22}/K_{20}$ *vs.* Re with the Schmidt number as parameter for $\lambda = 2$,

10 and 100. Because these graphs tend to obscure differences in the small Reynolds number region the coefficients of λ^{-2} in (76) and (77) are given in table 1 as a function of Re for $Sc = 1{\cdot}0$ and 100. The dispersion coefficient has been tabulated for $\lambda = 2, 10, 15, 100, 860, 1000$, $Sc = 0{\cdot}1, 0{\cdot}5, 1{\cdot}0, 10{\cdot}0, 100, 560$, for several Reynolds numbers $\geqslant 0{\cdot}1$ elsewhere (Lin 1969). Figure 3 for $\lambda = 2$ demonstrates the large differences between the predictions of the two models for $\lambda = 2$. For

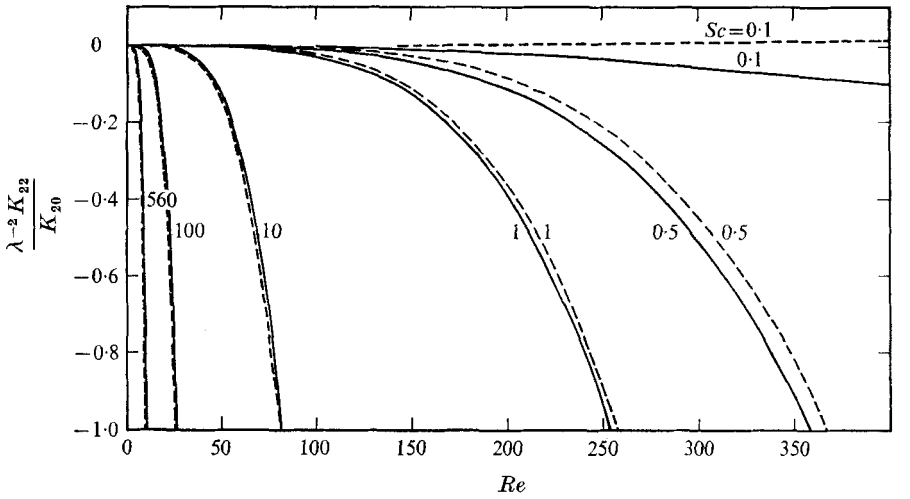

FIGURE 5. Curved tube correction to the dispersion coefficient normalized by the straight tube dispersion coefficient *vs.* Re for $\lambda = 100$ with Sc as a parameter. ———, Ergodan & Chatwin (1967); ———, this study.

model NLG the correction to the straight pipe dispersion coefficient is positive for small Reynolds numbers and then becomes negative as the Reynolds number increases for all Schmidt numbers. Note, for example, a 40 % increase in K_2 at $Sc = 0{\cdot}5$, $Re = 20$ and also that K_2 is decreased only if $Re > 30$. Figure 4 shows that this effect is still present at $\lambda = 10$ but to a less notable degree. This type of behaviour is not possible with model EC since for this model the dispersion coefficient is reduced by curvature if the Schmidt number is greater than

$$(33 \times 109/2569 \times 90)^{\frac{1}{2}} \simeq 0{\cdot}124.$$

Tabulated results indicate that $\lambda^{-2}K_{22}/K_{20}$ is positive for some range of Re at all Sc and λ, but that the magnitude may be so small as to be negligible. Thus on figure 5 for $\lambda = 100$ no significant increases in K_2 are shown.

Clearly, the curved pipe dispersion coefficient becomes increasingly different from the straight pipe result as the Reynolds number increases. The limitations of the straight pipe result as an approximation to the curved pipe solution can be inferred from figures 3 to 5. If one arbitrarily specifies the limit of the straight pipe as occurring when $|\lambda^{-2}K_{22}|/K_{20} \leqslant 0{\cdot}05$, the ranges of parameters listed in table 1 for the maximum values of the Re may be established as indicated. The values listed in table 2 again demonstrate that the differences between the two

models are at relatively small values of λ and are less pronounced at larger values of the Schmidt number. From table 2 it is clear that the straight pipe results are accurate over a larger range of Reynolds numbers for decreasing Sc at constant λ or for increasing λ at constant Sc.

	Coefficient of λ^{-2}	
Re	Equation (76)	Equation (77)
	$Sc = 1{\cdot}0$	
3	$0{\cdot}651507 \times 10^{-1}$	$-0{\cdot}974494 \times 10^{-6}$
6	$0{\cdot}434042 \times 10^{-1}$	$-0{\cdot}155919 \times 10^{-4}$
12	$0{\cdot}343671 \times 10^{-1}$	$-0{\cdot}249471 \times 10^{-3}$
18	$0{\cdot}263976 \times 10^{-1}$	$-0{\cdot}126294 \times 10^{-2}$
24	$0{\cdot}149435 \times 10^{-1}$	$-0{\cdot}399153 \times 10^{-2}$
30	$-0{\cdot}175084 \times 10^{-2}$	$-0{\cdot}974495 \times 10^{-2}$
36	$-0{\cdot}254791 \times 10^{-1}$	$-0{\cdot}202071 \times 10^{-1}$
42	$-0{\cdot}583371 \times 10^{-1}$	$-0{\cdot}374362 \times 10^{-1}$
48	$-0{\cdot}102773$	$-0{\cdot}638644 \times 10^{-1}$
54	$-0{\cdot}161601$	$-0{\cdot}102298$
	$Sc = 100$	
0·5	$0{\cdot}380660 \times 10^{-1}$	$-0{\cdot}763806 \times 10^{-5}$
1·0	$0{\cdot}387765 \times 10^{-1}$	$-0{\cdot}122209 \times 10^{-3}$
2·0	$0{\cdot}405248 \times 10^{-1}$	$-0{\cdot}195534 \times 10^{-2}$
3·0	$0{\cdot}385781 \times 10^{-1}$	$-0{\cdot}989893 \times 10^{-2}$
4·0	$0{\cdot}255909 \times 10^{-1}$	$-0{\cdot}312855 \times 10^{-1}$
5·0	$-0{\cdot}870353 \times 10^{-2}$	$-0{\cdot}763799 \times 10^{-1}$
6·0	$-0{\cdot}775058 \times 10^{-1}$	$-0{\cdot}158383$
7·0	$-0{\cdot}1969458$	$-0{\cdot}293424$
8·0	$-0{\cdot}386088$	$-0{\cdot}500568$
9·0	$-0{\cdot}666933$	$-0{\cdot}801813$
10·0	$-1{\cdot}06441$	$-1{\cdot}22209$

TABLE 1. A comparison of the coefficients of λ^{-2} in (76), the result of the present analysis and (77), the results of Erdogan & Chatwin (1967), as a function of Re for $Sc = 1{\cdot}0$ and 100

			Model NLG			
			Re_{max}			
$\lambda \backslash Sc$	0·1	0·5	1·0	10·0	100	560
2	0·1	0·1	0·1	0·1	0·1	0·1
10	—	41	37	13	0·1	0·1
100	—	156	118	38	12	11
860	—	—	—	110	35	5
			Model EC			
			Re_{max}			
$\lambda \backslash Sc$	0·1	0·5	1·0	10·0	100	560
2	—	29	19	—	—	—
10	—	58	39	12	4	—
100	—	174	121	38	12	11
860	—	—	—	110	35	5

TABLE 2. Maximum values of the Reynolds number for which the straight pipe result predicts the dispersion coefficient in a curved pipe accurately. The criterion used is $|\lambda^{-2}K_{22}|/K_{20} \leqslant 0{\cdot}05$

One of the most striking results shown in figures 3 to 5 is the limitation on the magnitude of the Reynolds number imposed by the constraint that $K_2 > 0$. This is due to the limitation on the number of terms available in the velocity distribution and demonstrates the need for the determination of higher order terms in the velocity distribution.

As discussed in § 2.4, the minimum time at which the dispersion model, equation (42), applies is finite and within the range of practical interest for straight tubes and channels. Also (39) gives the points concentration when (42) holds. It is expected that similar behaviour will be found for curved systems and therefore it is possible to develop an approximate expression for the minimum time. The dispersion model fails to satisfy the condition at the entrance exactly, equation (27), except as $\tau \to \infty$. However, in the region of validity of the dispersion model this condition will be satisfied to a good approximation for finite τ and it can be demonstrated that if

$$\left| f_{1\max} \left(\frac{\partial \bar{C}}{\partial X_1} \right)_{x=0} \right| \leqslant 10^{-7}, \tag{78}$$

where $f_{1\max}$ is the largest value of f_1 assumed at any transverse location, is used as a criterion for determining the minimum time an excellent approximation of the results obtained from exact solutions for straight tubes and channels can be generated. Applying this criterion to curved tubes yields, within limitations to be described below,

$$\tau_{\min} \gtrsim 101 K_2^{0.9}. \tag{79}$$

For example, with $\lambda = 2$, $Sc = 0{\cdot}5$ and $Re = 20$, $K_2 = 0{\cdot}0212$ and (79) yields $\tau_{\min} \gtrsim 3{\cdot}2$. It is worth noting that (79) also yields a reasonable estimate for straight tubes for all Péclet numbers.

In developing (79) two factors were taken into account. First, the results as $K_2 \to 0$ are uncertain because of the necessity to truncate the expansion for K_2 as a one-term correction to the straight tube case. Second, the most interesting practical results given here are for Schmidt numbers characteristic of gases (0·5, 1·0) and liquids (100, 560). From these considerations (79) was developed so as to yield a maximum error of 13 % in estimating the $\tau_{\min}$ which satisfies (78) for Re less than the values shown in table 3.

$\lambda \backslash Sc$	0·1	0·5	1·0	10	100	560
2	20	20	20	14	5	2
10	60	60	48	20	8	3
100	210	210	204	72	24	10

TABLE 3. Maximum values of the Reynolds number for which $\tau_{\min}$ for curved tubes may be predicted from (79) within the restriction given by (78)

3.2. *Curved channel*

The curved channel dispersion coefficient given by (74) and normalized by dividing by the straight channel result given by Phillip (1963), see equation (80),

is plotted against λ, with the Péclet number as a parameter, in figure 6:

$$K_{\text{s.c.}} = \frac{1}{Pe^2} + \frac{2}{105}. \tag{80}$$

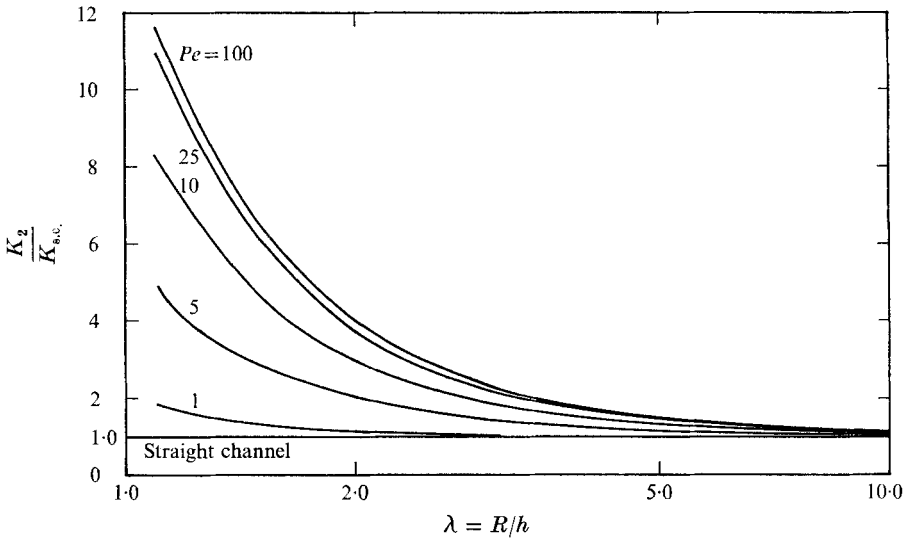

FIGURE 6. Normalized dispersion coefficient in a curved channel, $K_2/K_{\text{s.c.}}$, plotted against the curvature ratio λ, with the Péclet number as a parameter.

Since the velocity distribution is known exactly for the curved channel the dispersion coefficient is also exact. The lengthy expression for the dispersion coefficient is given by Lin (1969). Here the effect of curvature is only to increase the dispersion coefficient above that for straight channels. This is due to the asymmetry of the velocity profile since the effect is more pronounced at small values of λ, where the maximum velocity is closer to the inner wall. Solute moving at the maximum velocity in a curved channel has a shorter distance to move to reach any axial position than solute moving near the outer wall. Hence, relative to the straight channel the solute tends to spread out more, even though the maximum velocities in both systems are about the same. Thus the dispersion coefficient is larger for the curved system. The curve for $Pe = 100$ on figure 6 represents the situation when axial molecular diffusion is essentially negligible and so the curves for all larger Pe lie on that for $Pe = 100$. As the Péclet number is decreased at constant λ the ratio of the dispersion coefficients decreases because axial molecular diffusion contributes an increasingly larger fraction to the total dispersion effect. Furthermore, (74) and (80) reveal that for a given Péclet number molecular diffusion contributes a greater fraction of the total dispersion effect in flat plates than in curved channels.

Applying the criterion developed in § 3.1 for the minimum time for which the dispersion model applies to the curved channel system yields

$$\tau_{\min} \gtrsim 35 K_2^{0.92}. \tag{81}$$

This equation is a good approximation for all values of λ and Pe in the curved channel case and for all values of Pe in the straight channel.

It is important to note that the effect of curvature has been to markedly increase the dispersion coefficient for all values of the parameters for the curved channel. This is the opposite of the result obtained for curved tubes, where the theory predicts a decrease in the dispersion coefficient in curved systems for all but very small Reynolds numbers. This is due to the strong influence of radial mixing brought about by the secondary flow which is present in curved tubes but absent in curved channels. Although the asymmetry in the axial velocity is still present, this effect is evidently overcome by the secondary mixing in the radial direction as the Reynolds number increases such that the dispersion coefficient is decreased rather than increased in curved tubes.

4. Conclusions

The dispersion coefficient for laminar flow in curved tubes and channels has been determined analytically by a dispersion model which allows an accurate computation of the concentration distribution once the region of applicability of the model has been reached. The minimum time required for the dispersion model to apply has been estimated by an approximate procedure which is known to give accurate results in the case of straight tubes and parallel plate systems. In contrast to a previous analysis, it is found that the dispersion coefficient for curved tubes may be increased substantially above that for a straight tube with the same pressure gradient as that which exists along the centre-line of the curved tube, particularly at low Reynolds number flows in liquid systems. The mechanisms contributing to the behaviour of the dispersion as a function of the Reynolds number have been discussed, the main opposing factors being the asymmetric axial velocity distribution, which tends to increase dispersion, and the secondary flow, which decreases it.

Since the curved channel also has an asymmetrical axial velocity distribution but no secondary flow, dispersion is generally enhanced in the curved system as compared to the straight one.

This work was supported by the office of Saline Water, U.S. Department of Interior. The authors wish to acknowledge that the efforts of Dr P. C. Chatwin of the Department of Applied Mathematics, University of Liverpool, England were most helpful in arriving at the formulation given in § 2.1. The authors also acknowledge that Mr R. Sankarasubramanian suggested that the power-law form given in equation (79) would be a reasonable approximation to equation (78). The calculations were performed at the Clarkson College Computing Center.

Appendix

The full expressions for $w_2(y,\phi), L_1(y), L_{21}(y), G_2(y)$ and $H_{21}(y)$ are lengthy and are not given here. Detailed expressions for these functions will be provided by the authors upon request. The other functions mentioned but not given explicitly in the main body of the text are as follows.

$$w_0(y) = 1-y^2,$$

$$w_1(y,\phi) = w_{11}(y)\cos\phi = -\tfrac{3}{4}w_0(y)\cos\phi\,[1-(Re^2/8640)\,(19-21y^2+9y^4-y^6)]\,y,$$

$$w_2(y,\phi) = w_{20}(y)+w_{22}(y)\cos 2\phi,$$

$$w_{0m} = \tfrac{1}{2}, \quad w_{1m} = 0,$$

$$w_{2m} = -\frac{1541Re^4}{576^2\times 25\,200}-\frac{528Re^2}{5\times 576^2}+\frac{1}{96},$$

$$\psi_1 = \psi_{11}(y)\sin\phi = -\frac{Re}{288}w_0^2\sin\phi\,(4-y^2)\,y,$$

$$\psi_2 = \frac{Re}{5760}y^2w_0^2\sin 2\phi\left[(16-7y^2)-\frac{Re^2}{80640}\times(4979-2792y^2+777y^4-134y^6+5y^8)\right],$$

$$L_{11}(y) = (2Re^2/576)\,[Sc(y-\tfrac{13}{4}y^3+\tfrac{15}{4}y^5-\tfrac{7}{4}y^7+\tfrac{1}{4}y^9)+(\tfrac{19}{40}y-y^3+\tfrac{3}{4}y^5-\tfrac{1}{4}y^7+\tfrac{1}{40}y^9)]-2y(1-y^2),$$

$$G_{11}(y) = \frac{2Re^2}{576}\,[Sc(-\tfrac{17}{240}y+\tfrac{1}{8}y^3-\tfrac{13}{96}y^5+\tfrac{15}{192}y^7-\tfrac{7}{320}y^9+\tfrac{1}{480}y^{11})+(-\tfrac{4}{75}y+\tfrac{19}{320}y^3-\tfrac{1}{24}y^5+\tfrac{1}{64}y^7-\tfrac{1}{320}y^9+\tfrac{1}{4800}y^{11})]-\tfrac{1}{12}(-4y+3y^3-y^5),$$

$$L_1(y) = -\frac{Sc}{2y}\frac{d}{dy}[\psi_{11}(y)\,G_{11}(y)]+w_{20}(y)-w_{2m}-\tfrac{1}{2}yL_{11}(y)-\frac{1}{2y}\frac{d}{dy}[yG_{11}],$$

$$L_2(y) = -\frac{Sc}{2y}\left\{\frac{d}{dy}(\psi_{11}H_{21})+y\psi_{11}\frac{d}{dy}(g_{20})\right\}+[w_{20}+\tfrac{1}{2}yw_{11}-w_{2m}-\tfrac{1}{2}y^2w_{0m}]\,g_{10}+[w_{11}+wy_0-y]\,\tfrac{1}{2}G_{11}+(w_0-w_{0m})\,G_2+\tfrac{1}{2}yK_0-yL_{21}-\frac{y^2}{2}\nabla^2g_{20}-\frac{y}{2}\frac{d}{dy}(g_{20})-\frac{1}{2y}\frac{d}{dy}(yH_{21}),$$

$$\nabla^2g_{20} = \tfrac{1}{8}(-\tfrac{1}{8}+\tfrac{5}{6}y^2-\tfrac{5}{4}y^4+\tfrac{1}{2}y^6).$$

REFERENCES

Ananthakrishan, V., Gill, W. N. & Barduhn, A. J. 1965 *A.I.Ch.E. J.* **11**, 1063.

Chatwin, P. C. 1970 *J. Fluid Mech.* **43**, 321.

Dean, W. R. 1927 *Phil. Mag.* **4**, (7) 208.

Dean, W. R. 1928 *Phil. Mag.* **5**, (7) 673.

Erdogan, M. E. & Chatwin, P. C. 1967 *J. Fluid Mech.* **29**, 465.

Gill, W. N. 1967*a* *Proc. Roy. Soc.* A **298**, 335.

Gill, W. N. 1967*b* *Chem. Engng Sci.* **22**, 1013.

Gill, W. N. & Ananthakrishnan, V. 1966 *A.I.Ch. E. J.* **12**, 906.

GILL, W. N. & ANANTHAKRISHNAN, V. 1967 *A.I.Ch.E. J.* **13,** 801.

GILL, W. N., ANANTHAKRISHNAN, V. & NUNGE, R. J. 1968 *A.I.Ch.E. J.* **14,** 939.

GILL, W. N., GÜCERI, Ü. & NUNGE, R. J. 1969 *Office of Saline Water, R. & D. Progress Rep.* no. 443.

GILL, W. N. & SANKARASUBRAMANIAN, R. 1970 *Proc. Roy. Soc.* A **316**, 341.

GILL, W. N. & SANKARASUBRAMANIAN, R. 1971 *Proc. Roy. Soc.* A **322**, 101.

GOLDSTEIN, S. 1965 *Modern Developments in Fluid Dynamics*, vol. I, p. 315. Dover.

LIN, T.-S. 1969 M.S. thesis, Clarkson College of Technology.

MCCONALOGUE, D. J. 1970 *Proc. Roy. Soc.* A **315**, 99.

MCCONALOGUE, D. J. & SRIVASTAVA, R. S. 1968 *Proc. Roy. Soc.* A **307**, 37.

PHILIP, J. R. 1963 *Australian J. of Physics*, **16**, 286.

SANKARASUBRAMANIAN, R. & GILL, W. N. 1971 *Int. J. Heat Mass Transfer*, **14**, 905.

TAYLOR, G. I. 1953 *Proc. Roy. Soc.* A **219**, 186.

TAYLOR, G. I. 1954*a* *Proc. Roy. Soc.* A **223**, 446.

TAYLOR, G. I. 1954*b* *Proc. Roy. Soc.* A **225**, 473.

TOPAKOGLU, H. C. 1967 *J. Math. Mech.* **16**, 1321.